Biological and Medical Applications of Materials and Interfaces

Smart Fluorescent Hydrogel Glucose Biosensing Microdroplets with Dual-mode Fluorescence Quenching and Size Reduction

Hye-In Park, and Soo-Young Park

ACS Appl. Mater. Interfaces, **Just Accepted Manuscript** • DOI: 10.1021/acsami.8b10768 • Publication Date (Web): 22 Aug 2018

Smart Fluorescent Hydrogel Glucose Biosensing Microdroplets with Dual-mode Fluorescence Quenching and Size Reduction

*Hye-In Park and Soo-Young Park**

Department of Polymer Science & Engineering, Polymeric Nanomaterials Laboratory, School of Applied Chemical Engineering, Kyungpook National University, 80 Daehak-ro, Buk-gu, 41566 Daegu, Korea

*E-mail: psy@knu.ac.kr

Keywords: hydrogel, poly(acrylic acid), biosensor, glucose, microfluidics, carbon dot, glucose oxidase, horseradish peroxidase

Abstract: Fluorescent hydrogel glucose biosensor (FHGB) microdroplets were fabricated using a microfluidic method with glass capillaries having a coaxial flow-focusing geometry with cross-linked poly(acrylic acid) (PAAc) immobilized with carbon dots (CDs), glucose oxidase (GOx), and horseradish peroxidase (HRP) after the conversion of poly(acrylamide) to PAAc. The prepared FHGB droplets showed a dual response to glucose of CD fluorescence quenching and droplet size reduction upon bienzymatic reaction with glucose; the reaction of GOx and HRP with glucose produced gluconic acid and -OH radicals, which caused CD fluorescence

quenching and size reduction, respectively. These small FHGB droplets showed good sensitivity (linear range of ~30 mM with the limit of detection of 0.052 mM), high selectivity (against the main ingredients of human blood serum), and long stability (due to dry state during storage). These FHGB droplets were tested with human blood serum and they maintained sensing performance for a long time in the dry state. Thus, the FHGB droplets demonstrate a new method to detect glucose levels with small sample amounts by the dual-mode response. They can be further applied as implanted continuous-detection biosensor droplets because of their biocompatibility.

1. INTRODUCTION

Cross-linked polymer hydrogel networks are good candidates for smart materials if they respond to external stimuli through volume changes, because significant volume changes are possible in hydrogels with large amounts of absorbed water. Many synthetic hydrogels including poly(ethylene glycol), poly(acrylic acid) (PAAc), poly(vinyl alcohol), poly(acrylamide) (PAAm), and their derivatives have been used for smart material applications because of their relatively easy network formation and functionalization during synthesis compared to their natural hydrogel counterparts of polysaccharides and proteins.[1] Cross-linked polyelectrolytes are charged hydrogels because of their high hydrophilicity. Polyelectrolytes can be either strong or weak. The charge states of strong and weak polyelectrolytes are independent and dependent on pH changes, respectively. For example, PAAc, a weak anionic polyelectrolyte, becomes charged and swelled at high pH by deprotonation. Such hydrogels can be used for various applications.[2] For example, stimuli-responsive hydrogels have been used in microfluidic channels as valves to regulate flow without external control.[3-4] Porous-structured hydrogel microdroplets immobilized with receptor molecules can be used for the specific and efficient binding of analyte molecules[5] or capture of cellular secretions.[6] The biophysical similarity of hydrogels to soft biological tissues makes them widely applicable for 3D cell cultures, tissue engineering, and regenerative medicine.[7-8]

Nano-sized fluorescent materials, such as quantum dots (QDs) and carbon dots (CDs), have been applied as fluorophores. Over the past decade, considerable progress has been achieved in the synthesis and application of QDs, as well as in understanding their properties.[9-10] Based on their excellent optical properties, QDs have attracted wide attention and extensive research for biological applications. However, QDs require further modification for use in biological

applications as they are toxic, environmentally hazardous, susceptible to ultraviolet light excitation, easily photo-bleached, and chemically unstable.[11] In contrast, CDs, as another nano-sized carbon material, have recently received attention because of their good solubility in water, strong luminescence, high biocompatibility, ease of surface functionalization, long-term resistance to photo-bleaching, and low cost.[12-13] CDs can be synthesized by top-down and bottom-up methods.[14-24] Between them, the bottom-up method offers fast and simple access to many different CDs with varied surface functionalities and tunable properties. Aqueous CD solutions have been used for glucose biosensor applications by fluorescence quenching with enzymes.[25] For example, the enzymatic reaction of glucose oxidase (GOx) with glucose generates gluconic acid and H_2O_2.[26] The produced H_2O_2 can be decomposed into -OH radicals by horseradish peroxidase (HRP), and the gluconic acid decreases the local pH.[27] The -OH radicals cause the fluorescence quenching of CDs; therefore, the degree of quenching represents the amount of glucose. However, aqueous CD solutions are unstable and difficult for patients to carry in the field and use at home. Thus, solid-state biosensors are quite desirable for practical applications. The maximum quenching of CD occurs in aqueous media; thus, water-absorbed hydrogels are good solid matrix candidates for biosensor applications.

Uniform-sized hydrogel droplets can be generated rapidly in microfluidic channels with monomer or polymer solutions in the form of water-in-oil (W/O) droplets.[28] Flow-focusing and T-junction geometries with poly(dimethylsiloxane) (PDMS) and glass-capillary microfluidic chips are usually used for droplet production.[29] The dimensions of the microfluidic-chip channel and the flow-rate ratio of the two phases can be used to fine-tune the droplet sizes. These hydrogel droplets are mostly applied to the encapsulation of single molecules or cells, because they allow high-throughput analysis and manipulation with precise control of the local

environment.[30] Polyelectrolyte hydrogel droplets have also been studied for smart materials because of their pH responsiveness. For example, pH-responsive microdroplets of PAAc hydrogel were fabricated as W/O droplets with pH-dependent sizes.[31] These hydrogel droplets can be loaded with valuable materials, such as drugs, because of their high porosity in the swollen state, with drug release triggered by environmental pH changes (in acidic environment) in the shrunken state. PAAc can be easily functionalized with its pendant carboxylic groups, which can couple with amine-containing materials through the N-(3-dimethylaminopropyl)-N′-ethylcarbodiimide (EDC) coupling agent. Fluorescent PAAc can be fabricated by immobilizing CDs (which have many functional groups, including amine groups, when CDs are made from amine-containing materials such as ethylene diamine via the bottom-up method) through EDC coupling. These fluorescent PAAc microdroplets can be applied in small biosensors by immobilizing GOx and HRP. These fluorescent hydrogel glucose biosensor (FHGB) droplets are quenched by -OH radicals and the droplet size is decreased by a bienzymatic reaction of GOx and HRP; therefore, these FHGB droplets can be used as dual-mode glucose biosensors. Small-sized FHGB droplets are advantageous for small sample volumes. They also can be used for sensing glucose in small confined areas, providing data for localized and not large-averaged regions. In addition, they can be stored in the dry state and used in water whenever needed.

In this work, FHGB droplets were fabricated with cross-linked PAAc after the immobilization of CD, GOx, and HRP using a microfluidic method with glass capillaries having a coaxial flow-focusing geometry after the conversion of PAAm to PAAc. The produced uniform-sized polyelectrolyte droplets responded to glucose by the dual modes of fluorescence quenching and size reduction. This dual response of the FHGB droplets, monitored with simple optical microscopy, permitted doubly checkable glucose sensing. The dry solid-state droplets could be

stored for long periods and used whenever needed. Thus, these FHGB droplets demonstrate a new method for detecting glucose levels from small samples; they can be further applied in implanted continuous-detection biosensor droplets because of their biocompatibility.

2. EXPERIMENTAL

2.1. Materials

Acryl amide (AAm, Junsei, Japan), *N,N′*-methylenebis(acrylamide) (MBAm, TCI, Japan), ammonium persulfate (APS, Duksan, South Korea), *N*-hydroxysuccinimide (NHS, Sigma-Aldrich), *N*-(3-dimethylaminopropyl)-*N′*-ethylcarbodiimide hydrochloride (EDC·HCl, Sigma-Aldrich), D-(+)-glucose, glucose oxidase (GOx, Sigma-Aldrich), L-ascorbic acid (Sigma-Aldrich), urea (Sigma-Aldrich), dopamine (Sigma-Aldrich), lactose (Sigma-Aldrich), sodium chloride (Duksan, South Korea), human blood serum (Sigma-Aldrich, USA), horseradish peroxidase (HRP, Sigma-Aldrich), sodium hydroxide (NaOH, Duksan, South Korea), fluorocarbon oil (NovecTM7500, 3M, USA), Krytox 157FSH (Dupont, USA), silicone oil (5 cSt, 100 cSt, SO, Shin-Etsu, Japan), tetramethylethylenediamine (TEMED, Sigma-Aldrich), citric acid (CA, Sigma-Aldrich), tetraethyl orthosilicate (TEOS, TCI, Japan), and ethylene diamine (EDA, Daejung, South Korea) were used as received. pH buffer solutions were obtained from Duksan, South Korea. Deionized (DI) water was used after purification on a reverse osmosis system (PureRO, Romax, South Korea).

2.2. Preparation of CD

CDs were prepared according to a previously reported method with a slight modification using a mini bench-top reactor (4566, MK Science, South Korea).[32] Briefly, CA (0.4 g) and EDA (270 μL) were dissolved in DI water (80 mL). Then, the mixed solution was transferred to a sealed

reactor (200 mL) and heated at 200 °C for 4 h. After the reaction, the reactor was cooled to room temperature (20 °C) in air. The product, which was brown-red and transparent, was subjected to dialysis in order to obtain pure CDs. After the dialysis process, the final concentration of the resultant CD solution was approximately 5.8 mg/mL, which was calculated from the solid weight after complete drying. Detailed fluorescence properties can be found in our previous papers.[33-34]

2.3. Microfluidics

A micro-capillary device consisting of a tapered-round glass capillary enclosed in a square glass capillary was used to prepare the hydrogel droplets (Figure S1). The square capillary (Vitrocom, USA, 0.9 mm × 0.9 mm) was used without any surface treatments. The round glass capillary (Vitrocom, USA, 0.7 mm inner diameter (ID) × 0.87 mm outer diameter (OD) × 100 mm length) was tapered in half using a Micropipette Puller (P-97, Sutter Instrument, USA). Hydrophilic coating was performed with TEOS as follows. The round capillary was washed with ethanol and DI water, dried at 85 °C for 10 min, and treated with oxygen plasma for 5 min using a plasma system (FC-10005, Femto Science, South Korea). The treated capillary was inserted in a vial containing 5 wt% TEOS in ethanol for 30 min, washed with ethanol and DI water, and finally dried in an oven at 70 °C for 15 min. The OD of the round capillaries (0.87 mm) was comparable to the ID of the square capillary (0.9 mm), such that a round capillary could be inserted into the square capillary to achieve tight fitting and coaxial alignment. The diameter of the tapered end was ~80 μm. To prepare hydrogel single droplets, aqueous AAm monomers (5 M) and a cross-linker of MBAm (0.15 M) with APS (0.05 M) was flowed through the central tapered round capillary as the disperse phase, while the outer fluorocarbon oil (Novec 7500) containing TEMED (0.5 wt%) and the fluorinated surfactant (Krytox 157FSH, 2 wt%) were flowed in the same direction in the squared capillary as a continuous phase to produce W/O

single droplets in a coaxial co-flow geometry. The fluorocarbon oil squeezed the aqueous AAm monomer solution into monodisperse droplets. TEMED was dissolved in the continuous phase as an accelerator for AAm polymerization, and APS in the disperse phase functioned as an initiator for AAm polymerization. The prepared PAAm droplets were polymerized at 100 °C by post-heat treatment in a 50-mL vial. The flow rates were controlled using a pneumatic microfluidic flow-rate control system (OB1 pressure controller, Elveflow, France), which was capable of pumping two fluids at two different velocities. These systems were connected to the microcapillary device using shrinkable connector tubes (Tommyheco, Korea, 2.38 mm × 1.59 mm × 2.38 mm) and flexible plastic tubing (Norton, 0.51 mm ID, 1.52 mm OD). By pumping air gas at a finely controlled rate into the vials containing the liquids, the Elveflow unit pressurized the vials, which caused the fluids to flow through the tubes and into the device. The typical pressures of the inner and outer fluids were 10 and 130 mbar, respectively.

2.4. Preparation

The produced PAAm hydrogel droplets (1 g, in a 20 mL vial) were converted to FHGB droplets by immersing them in an aqueous solution of NaOH (3 M, 13.5 mL) in the presence of TEMED (10 vol%, 1.5 mL), followed by magnetic stirring for 12 h; washing with DI water; activating with EDC/NHS (0.2 M/0.2 M, 2 mL) for 5 h; immobilizing with CDs (0.58 mg/mL, 5 mL), GOx (45 μM), and HRP (15 μM) for 12 h; and magnetic stirring for 12 h, as shown in Scheme 1.

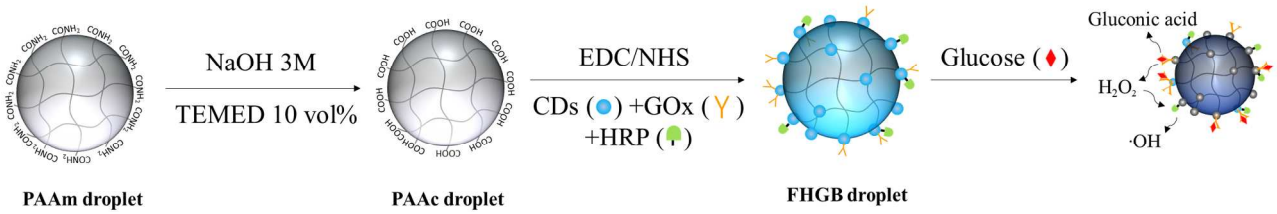

Scheme 1. Schematic of preparation of the FHGB droplets.

2.5. Measurements

Surface images of the FHGB droplets were obtained using a field-emission scanning electron microscope (FE-SEM, SU8220, Hitachi, Japan) that was operated at accelerating voltage of 15 kV. Samples for SEM were freeze-dried using a freeze dryer (FD-1000, Rikakikai, Japan), and coated with platinum using a coater. Attenuated total-reflection Fourier-transform infrared (ATR-FTIR) spectra were obtained with FTIR spectroscopy (FT/IR-4100, Jasco, Japan) in the range 600–4,000 cm^{-1} at a resolution of 4 cm^{-1} by collecting the average of 64 scans. Hydrogel droplets were observed during production in the microfluidic channel with a high-speed charge-coupled device (CCD) camera (STC-TC83USB-AS, Sentech, Japan) on an optical microscope (JSP-20T, Samwon, South Korea). Bright-field images of the droplets on the glass container after production were taken with an optical microscope (ANA-006, Leitz, Germany). After the reaction of the FHGB droplets with glucose, the pH of the solution was measured using a pH meter (YK-2001PHA-pH/EC, Sechang, South Korea). The fluorescence of the hydrogel droplets immobilized with CDs was studied with a fluorescence microscope (E600POL, Nikon eclipse, Japan). The ultraviolet–visible (UV-Vis) and photoluminescence (PL) spectra were recorded on a UV-Vis spectrophotometer (UV-2401 PC, Shimadzu, Japan) and spectrofluorophotometer (RF-5301PC, Shimadzu, Japan), respectively. The PL spectra were recorded using a specially

designed cell for FHGB droplets, as shown in Figure S2. Photographic images of the FHGB droplets were obtained with a smartphone camera (SM-G925S, Samsung, South Korea).

3. RESULTS AND DISCUSSION

3.1. Preparation of hydrogel droplets

Uniform droplets were successfully produced in the microfluidic channel, as shown in Movie S1. The droplet sizes were controlled by the pressures of the continuous (P_c) and disperse (P_d) phases. For example, stable uniform droplets are produced in the P_c range 40–160 mbar at P_d = 10 mbar (Region III in Figure 1(a)), although the pressure value is dependent on the size of the glass capillary orifice in this pressure-control pump. As P_c is increased from 40 to 160 mbar, the diameter of the droplet decreases from 571 to 363 μm, as shown in Figure 1(a). In other pressure ranges (Regions I and II in Figure 1(a)), the sizes of the produced droplets are not uniform because of the jetted regime, or droplets could not be produced, as shown in Figure 1(b). Thus, we can control the droplet size by finely controlling the pressures of both the disperse and continuous phases.

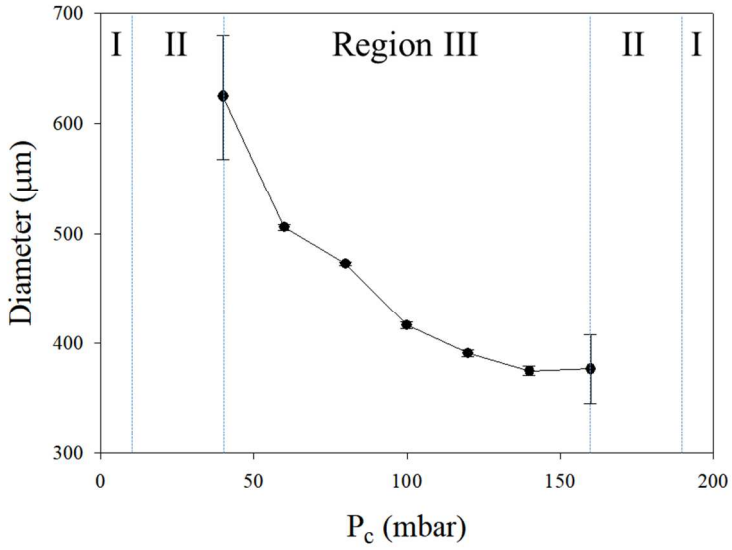

(a)

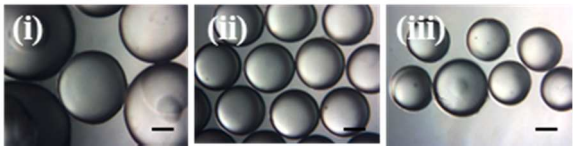

(b)

Figure 1. (a) Diameter of the PAAm hydrogel droplets as a function of P_c at fixed P_d = 10 mbar; Regions I, II, and III represent no, non-uniform, and uniform droplets, respectively. (b) Photographic images of the PAAm droplets produced at P_c = (i) 30, (ii) 120, and (iii) 170 mbar with a fixed P_d = 10 mbar; scale bars are 200 μm.

The produced PAAm hydrogel droplets were changed to PAAc hydrogel droplets by NaOH treatment in the presence of TEMED,[35] and the PAAc hydrogel droplets were further functionalized with CD, GOx, and HRP to yield FHGB droplets. In order to confirm the conversion from PAAm to PAAc and the immobilization of CD, FTIR spectroscopy is performed, as shown in Figure 2. The FTIR spectrum of the PAAm (Figure 2(a)) shows a NH_2 stretching band at 3193 cm^{-1}.[36] After the conversion of PAAm to PAAc (Figure 2(b)), the NH_2

stretching band at 3193 cm^{-1} decreases significantly; new peaks appear at 1410 and 1562 cm^{-1}. These peaks arise from the symmetric and antisymmetric stretching bands of the carboxylate ion (COO^-), respectively.[37] Thus, the amine groups of PAAm are successfully converted to carboxylic groups, although the shoulder at 3193 cm^{-1} indicates that small amounts of amine groups remain. After the immobilization of the CDs (Figure 2(c)), the peaks of the symmetric and antisymmetric stretching bands of the carboxylate ion (COO^-) at 1410 and 1562 cm^{-1} are decreased, whereas the new peaks at 2536 and 1292 cm^{-1} corresponding to OH stretching[38] and amide II bonds[39], respectively, are observed. These new peaks are from the immobilized CDs and the amide bonds through EDC coupling, respectively. To verify whether CD, GOx, and HRP were covalently immobilized in the droplets, the water into which the droplets were inserted was tested. Figure S3(a) displays the UV spectra of pure water, the aqueous CD (0.58 mg/mL) and GOx/HRP (3:1 mole ratio, 3 wt%) solutions, and water 2 h after immersion of 0.1 g FHGB droplets in 4 mL water. The UV spectrum of the aqueous CD solution showed peaks at 350 nm and that of the aqueous GOx/HRP mixture solution showed peaks at 410 and 470 nm. However, the UV spectrum of the water in which the FHGB droplets were immersed showed no peaks, indicating that the enzymes were firmly immobilized in the FHGB droplets. These FHGB droplets emitted a blue color when exposed to UV at 365 nm, as shown in Figure S3(b). Figure S4 shows the PL spectra of FHGB droplets at CD concentrations of 5.8, 0.58, and 0.058 mg/mL. The intensity of the PL spectrum at 5.8 mg/mL is saturated, whereas the intensity at 0.058 mg/mL is too low. Therefore, 0.58 mg/mL was chosen as the CD concentration. Figure S5 is a plot of Q_f for the CD (0.58 mg/mL)/GOx/HRP aqueous solution, as a function of the mole ratio between GOx and HRP at a constant concentration (34 μM) of GOx + HRP. Q_f increases with

the mole ratio until a GOx/HRP mole ratio of 2.5, at which point Q_f reaches saturation. Thus, for subsequent experiments, we used a CD aqueous solution with a 3:1 mole ratio of GOx/HRP.

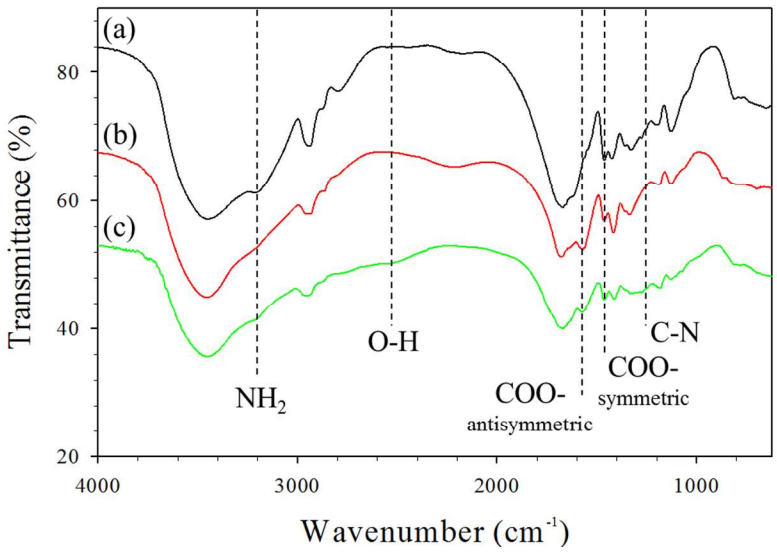

Figure 2. FTIR spectra of (a) PAAm, (b) PAAc, and (c) CD-immobilized PAAc droplets.

3.2. pH-responsive FHGB droplets

PAAc is a typical pH-responsive weak polyelectrolyte; therefore, the size of the FHGB droplets should be dependent on pH. The ratio of the droplet diameter (D/D_o) where D is diameter at certain pH and Do is the largest diameter was compared due to small size differences in initial droplets. Figure 3(a) plots the diameter ratio of the FHGB droplet in water as a function of pH. The diameter ratio of ~0.6 below the pKa of the carboxylic groups (pH = 2, 3, 4) is increased stepwise to ~0.9 at pH = 5, although the diameter ratio increases somewhat after this point, reaching 1 at pH = 12. Thus, the carboxylic groups of PAAc are deprotonated and become ionized to be repulsive and swelled after pKa; the volume of the droplet is increased by more than five times after pKa. Figure 3(b) depicts the diameter ratio change of the PAAc droplet at alternating pH 2 and 12 as a function of the cycle number. The diameter ratio is changed from

0.55 to 1 as the pH is changed from 2 to 12 for 10 cycles. The diameter ratios at each cycle are almost constant, indicating that the expansion and shrinkage of the FHGB droplet is quite stable. We did not perform further experiments for additional cycling, although we believe that the size change of the FHGB droplet would continue stably for further cycles. The diameter ratio of the PAAc droplet displayed little difference from that of FHGB at different pH values (Figure S6 (b)), indicating that deprotonation of carboxylic groups of PAAc and FHGB droplets occurs with similar dependency on pH. However, pH responsiveness does not occur with PAAm as shown in Figure S6 (a), which is strong evidence for the conversion of PAAm to PAAc.

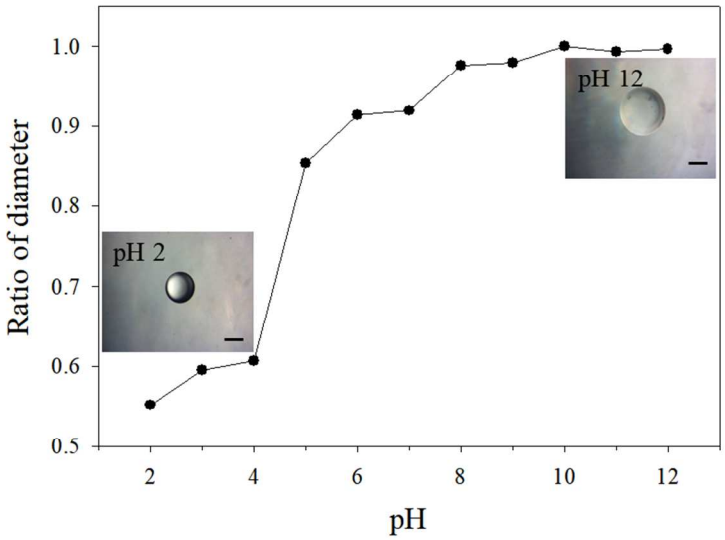

(a)

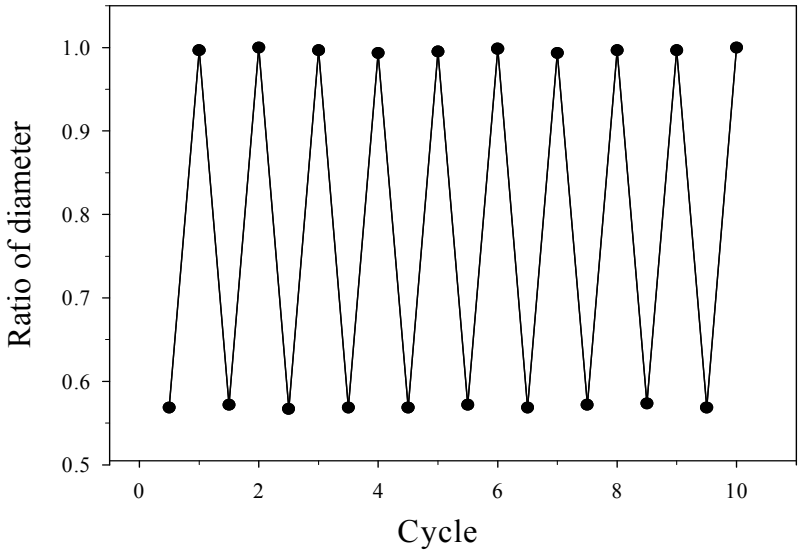

(b)

Figure 3. (a) Diameter ratio (D/D_o where D is diameter at certain pH and D_o is the largest diameter) of the FHGB droplet in water as a function of pH; the insets are photographic images at pH = 12 (upper right corner) and 2 (lower left corner), in which the scale bars are 200 μm; (b) diameter ratio of the FHGB droplet at alternating pH 2 and 12 as a function of cycle number.

3.3. Glucose detection of the FHGB droplets

The speed of glucose detection was tested with the FHGB droplets. Figure 4(a) provides the PL spectra of the FHGB droplets (0.05 g) in the glucose solution (30 mM, 2 mL) at different time intervals after the glucose solution was added to the vial; the insets show photographic fluorescence images of the droplets. Figure 4(b) depicts the degree of quenching ($Q_f = (F-F_0)/F_0$, where F_0 and F are the PL intensities at 450 nm without and with glucose, respectively, when excited at 360 nm) and their sizes; the insets are photographic images of the droplets with measured pHs in aqueous media. The Q_f continuously increases until ~5 h and then remains

almost constant. The real photographic fluorescence images show distinct fluorescence quenching 5 h after glucose addition, as shown in the insets of Figure 4(a), indicating that the presence of glucose can be detected by the naked eye. The diameter of the droplet decreases in opposition to the Q_f and the pH of the aqueous medium continuously decreases to 4.2 (see insets in Figure 4(b)). This result indicates that the size reduction of the droplet is caused by the production of gluconic acid by the reaction of GOx with glucose. The role of the enzyme in the FHGB droplet is confirmed by comparison with the hydrogel droplet immobilized only with CDs. Figure 4(c) shows the fluorescence images of the PAAc hydrogel droplets immobilized only with CDs compared to those of the FHGB droplets before and after glucose aqueous solution is added to the cell. Both droplets show similar fluorescence before glucose addition, whereas only the FHGB droplets show significant fluorescence quenching and size reduction after glucose addition. Thus, the bienzymatic reaction with glucose changes the fluorescence of the CDs as well as the droplet size. This dual-mode detection of glucose by fluorescence quenching and size reduction increases the visibility of glucose sensing by the naked eye. Further experiments for glucose biosensor application with the FHGB droplets were performed for more than 5 h after glucose aqueous solution addition.

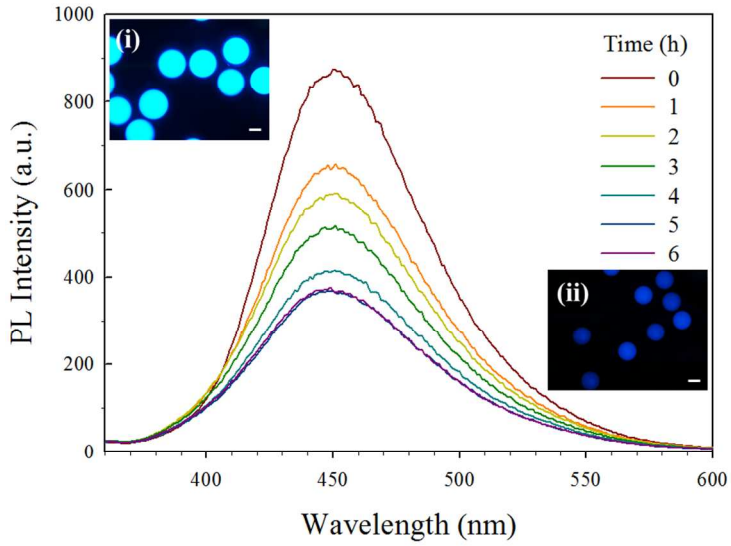
PL Intensity (a.u.)
Wavelength (nm)
Time (h)
0
1
2
3
4
5
6
(i)
(ii)

(a)

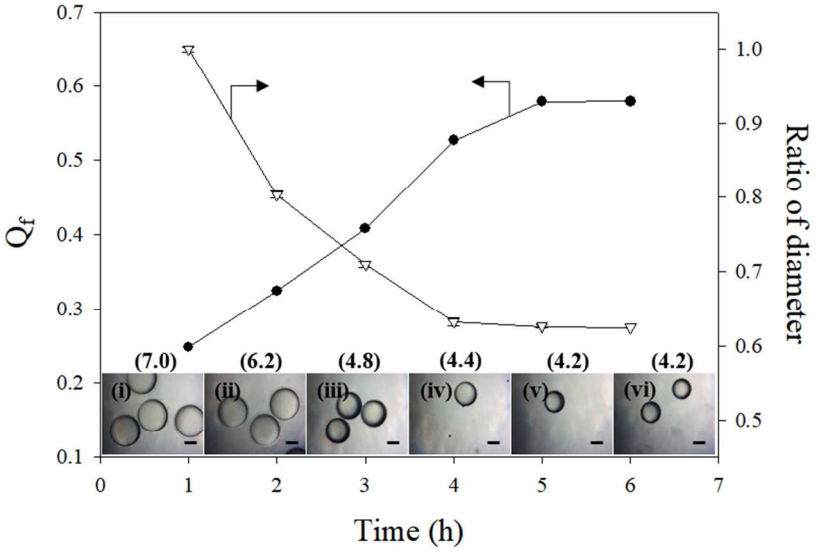
Qf
Ratio of diameter
Time (h)
(7.0)
(6.2)
(4.8)
(4.4)
(4.2)
(4.2)
(i)
(ii)
(iii)
(iv)
(v)
(vi)

(b)

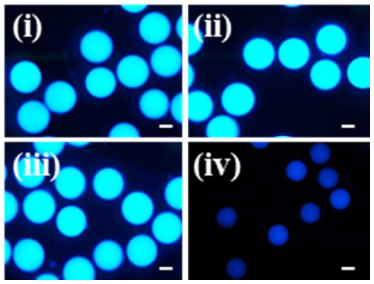
(i)
(ii)
(iii)
(iv)

(c)

Figure 4. (a) PL spectra of the FHGB droplets (0.05 g) in the glucose solution (30 mM, 2 mL) at different times after the glucose solution was added to the vial; insets are the fluorescence images (i) before and (ii) 5 h after glucose addition; scale bars in insets are 200 μm. (b) (Left axis) Q_f and (right axis) diameters of the FHGB droplets (0.05 g) in the glucose solution (30 mM, 2 mL) as a function of time after the glucose solution was added to the vial; insets are the bright-field images (i) before and (ii) 1, (iii) 2, (iv) 3, (v) 4, and (vi) 5 h after glucose addition; the numbers in parentheses show the solution pH, and (c) fluorescence images of (i, ii) the PAAc hydrogel droplets (0.05 g) immobilized only with CD (0.58 mg/mL, 5 mL) and (iii, iv) FHGB droplets (i, iii) before and (ii, iv) after glucose aqueous solution (30 mM, 2 mL) was added to the cell; all scale bars in (a, b, c) are 200 μm.

3.4. Performance of glucose detection of the FHGB droplets

The sensitivity, selectivity, and stability of glucose detection were tested with the FHGB droplets. First, the sensitivity of the FHGB droplets was studied. Figure S7(a) contains the PL spectra of the FHGB droplets (0.05 g) in glucose solutions (2 mL) at different glucose concentrations (C_gs). As C_g increased, the fluorescence intensity was continuously decreased to the level of 30 mM and thereafter remained constant. Figure S7(b) plots Q_f as a function of C_g. The linear range is ~30 mM with the limit of detection (LOD) of 0.0516 mM. LOD was calculated as 3 times standard deviation divided by the regression slope, where the standard deviation and the slope are derived from Figure S7 (b).[40] Next, the selectivity of the FHGB droplets was studied. Figure 5(a) compares the Q_f of the FHGB droplets (0.05 g) after 30 mM of urea, ascorbic acid, dopamine, lactose, NaCl, and glucose aqueous solutions (2 mL) are added to the cell. The Q_fs of all analytes except glucose show low values <0.03, indicating that

fluorescence quenching does not occur except with exposure to glucose (Q_f of glucose = 0.82). The dopamine and glucose mixture also shows a Q_f similar to glucose alone, indicating that other materials do not interfere with glucose detection, which is due to the strong selectivity of the GOx enzyme. Thus, the FHGB droplets are highly selective to glucose. In addition to the fluorescence quenching, the size of the droplet is another indicator for glucose detection. The sizes of the droplets in the analyte solutions are nearly constant at ~555 μm, near the original size of the droplet (560 μm), except for those in the ascorbic acid and glucose aqueous solutions. The ascorbic acid aqueous solution has the low pH of 4.1; therefore, the FHGB droplets shrank in the ascorbic acid solution. The FHGB droplet in the glucose aqueous solution also shrank because of the gluconic acid produced through GOx reaction with glucose, as mentioned previously. Lastly, the stability of the FHGB droplets was studied. The stability of the oven-dried FHGB droplet was tested after storing in the dry state for an extended period of time. Figure 5(c) depicts the fluorescence images of the FHGB droplets in the dry state and the swollen state in water with and without 30 mM glucose four weeks after drying. The FHGB droplets in the dry state shows high fluorescence intensity (Figure 5(c) (i)) and those in the swollen state in water without glucose four weeks after drying do not lose their intensity (Figure 5(c) (ii)). However, the FHGB droplets in the swollen state in water with glucose were quenched at almost the same level as those immediately after drying, where the Q_f after drying (Q_f = 0.55) was slightly lower than that of fresh FHGB droplets (Q_f = 0.58) (Figure 5c (iii)). The original PL spectra before and after glucose addition are shown (Figure S8). Thus, the FHGB droplet can remain in the dry state for use whenever needed.

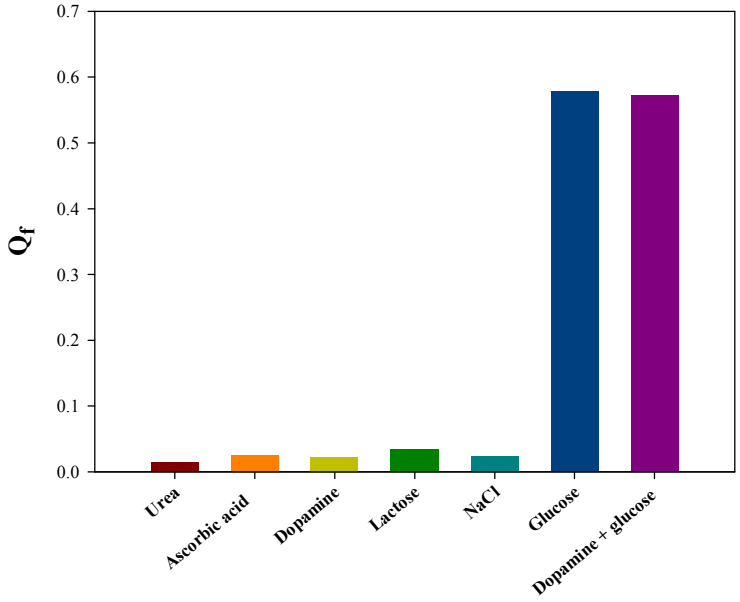
0.7
0.6
0.5
0.4
0.3
0.2
0.1
0.0
Q_f
Urea
Ascorbic acid
Dopamine
Lactose
NaCl
Glucose
Dopamine + glucose

(a)

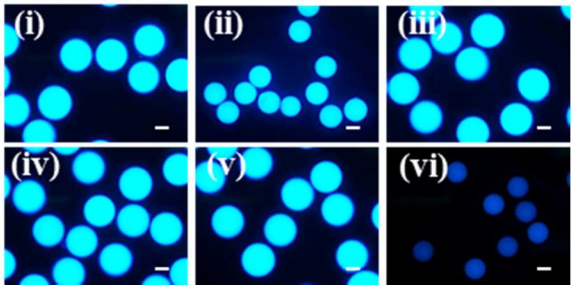
(i)
(ii)
(iii)
(iv)
(v)
(vi)

(b)

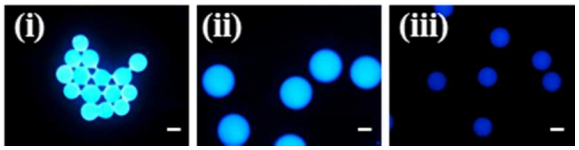
(i)
(ii)
(iii)

(c)

Figure 5. (a) Q_f of the hydrogel biosensor droplets (0.05 g) after (i) urea, (ii) ascorbic acid, (iii) dopamine, (iv) lactose, (v) NaCl, and (vi) glucose aqueous solutions (30 mM, 2 mL) are added to the cell, (b) fluorescence images of (a), and (c) fluorescence images of the FHGB droplets in (i) the dried state, and (ii, iii) the swollen state in water (ii) without and (iii) with 30 mM glucose four weeks after drying; all scale bars in (b, c) are 200 μm; the PL spectra in (a) were obtained following 5 h of incubation.

3.5. Morphology of the FHGB droplets

The morphologies of the freeze-dried and oven-dried FHGB droplets were studied and compared. Figures 6(a) and (b) compare the SEM images of the FHGB droplets freeze-dried at pH 7 (pure DI water) and 2 (buffer solution), respectively. Clear open structures are observed in the freeze-dried samples and the diameters of the droplets freeze-dried at pH 7 and 2 are 355 and 247 μm, respectively. These results indicate that water easily infiltrates the hydrogel droplet in water and that droplets at high pH have more open structures than those at low pH. However, the droplet dried in an oven at 60 °C is compact and closed compared to the freeze-dried samples (Figure 6c). Thus, the compact and closed structure is easily changed into the swelled and open structure when the droplets are inserted in water, and the pore size can be easily controlled by the pH.

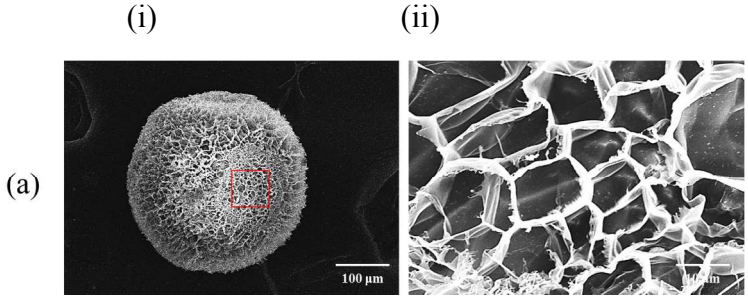

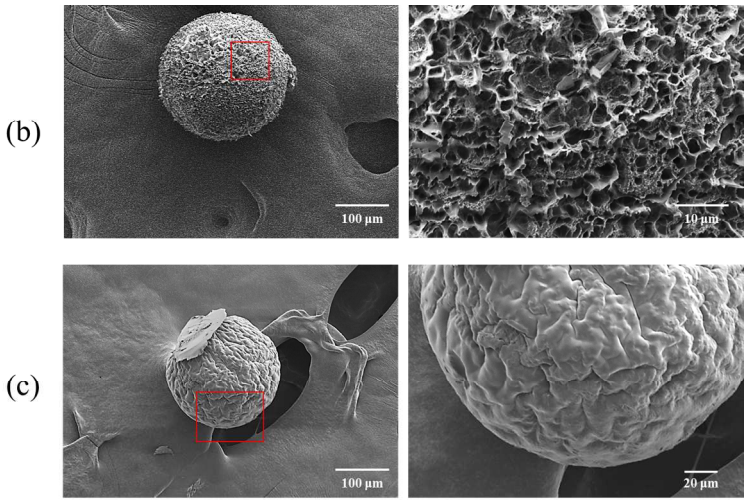

Figure 6. SEM images of (a, b) FHGB droplets freeze-dried at pH (a) 7 and (b) 2, and (c) FHGB droplet dried in an oven at 60 °C. (i) Low magnification and (ii) high magnification of the region of the red squares in (i).

Finally, we tested the ability of the FHGB droplets to detect glucose in diluted human blood serum (× 10 with DI water). The original amount of glucose in the human blood serum was 5.3 mM as measured by high-performance liquid chromatography (HPLC).[41] Thus, known amounts of glucose were added to the serum samples after centrifugation to remove large molecules. The glucose contents in the spiked serum samples were determined from the fluorescence spectra of the FHGB droplets using the calibration curve (Figure 5(a)). Table 1 shows the added and measured amounts of glucose in human blood serum. The recovery ratios (measured glucose)/(original glucose + added glucose) × 100 %) of 95.6, 108.6, 96.6, and 102.3% were obtained for serum samples at C_g (added glucose concentrations) of 0, 0.47, 1.47, and 9.47 mM, respectively, with the FHGB droplets (0.05 g) in water (2 mL), indicating that the FHGB droplets can be used with real human blood samples. Although small deviations from 100% were

observed, possibly reflecting interference by other biomaterials in human serum, these deviations were relatively small.

Table 1. Amounts of glucose in human blood plasma measured with the FHGB droplets

Samples	Glucose (mM)			Recovery[b] (%)	RSD[c] (n =5, %)
	Original[a]	Added	Measured		
1.	0.53	0	0.49	93.6	3.91
2.	0.53	0.47	1.10	110.4	3.76
3.	0.53	1.47	1.92	96.6	6.07
4.	0.53	9.47	10.03	100.3	4.61

[a]Original amount of glucose in human blood serum, [b]Recovery = (measured glucose)/(original glucose + added glucose) × 100%, [c]RSD is the relative standard deviation

4. CONCLUSION

The FHGB droplets showed pH responsiveness such that the droplets were swelled significantly above the carboxyl pKa (4.3). The swollen porous hydrogel droplets provided good aqueous environments for glucose sensing. The FHGB droplets exhibited good sensor performance by fluorescence quenching in terms of sensitivity, selectivity, and stability. Fluorescence quenching arose from the GOx/HRP reaction, which produced –OH radicals by a bienzymatic reaction. The sensor linear range and LOD were ~30 mM and 0.0516 mM, respectively. The fluorescence quenching was highly selective to glucose among the major ingredients of human blood. The dry FHGB droplets could be stored for long periods and maintain the same biosensing quality when used. In addition to fluorescence quenching as a sensor indicator, the size of the droplets was another sensor indicator of glucose, because the

gluconic acid produced by GOx reaction with glucose decreased the pH and caused the size reduction of the FHGB droplet. The size reduction was also selective to glucose, as well as acidic ingredients such as ascorbic acid. Thus, this dual-mode detection of glucose from fluorescence quenching and size reduction increased the visibility of glucose sensing by the naked eye. Small-sized FHGB droplets are advantageous when only small amounts of samples are available. The FHGB droplets can be used for sensing in small confined areas to provide localized, rather than large-area averaged data. The FHGB droplets can be stored in the dry state and used in water whenever needed. Thus, these FHGB droplets provide a new method to detect glucose levels; they could be further applied in implanted continuous-detection biosensor droplets because of their biocompatibility.

ASSOCIATED CONTENT

Supporting Information. The Supporting Information is available free of charge on the ACS Publications website at DOI:

Schematic and real photographic images of experimental setup; FHGB droplets sample holde; UV spectra of GOx/HRP and water after FHGB droplets immersion; photographic images of the FHGB droplets in a vial before and after exposure to UV light and PL spectra of the FHGB droplets in glucose solutions at different C_gs; PL spectra of the FHGB droplets at different CD concentrations; Q_f for the CD/GOx/HRP aqueous solution; Diameter ratio of the PAAm and PAAc droplets in water as a function of pH; PL spectra of FHGB droplets in the swollen state in water 4 weeks after drying (PDF)

Movie of production of FHGB droplets using microfluidics (AVI)

AUTHOR INFORMATION

Corresponding Author

*E-mail: psy@knu.ac.kr

Author Contributions

The manuscript was written through contributions of all authors. All authors have given approval to the final version of the manuscript.

ACKNOWLEDGMENTS

This work was supported by the National Research Foundation of Korea (2017R1A2B2006818)

Notes

The authors declare no competing financial interest.

REFERENCES

1. Larraneta, E.; Henry, M.; Irwin, N. J.; Trotter, J.; Perminova, A. A.; Donnelly, R. F., Synthesis and Characterization of Hyaluronic Acid Hydrogels Crosslinked using a Solvent-Free Process for Potential Biomedical Applications. *Carbohydr. Polym.* **2018,** *181*, 1194-1205.

2. Noh, K. G.; Park, S. Y., Biosensor Array of Interpenetrating Polymer Network with Photonic Film Templated from Reactive Cholesteric Liquid Crystal and Enzyme-Immobilized Hydrogel Polymer. *Adv. Funct. Mater.* **2018**, 1707562.

3. Eddington, D. T.; Beebe, D. J., Flow Control with Hydrogels. *Adv. Drug Delivery Rev.* **2004,** *56* (2), 199-210.

4. Park, K. S.; Kim, C.; Nam, J. O.; Kang, S. M.; Lee, C. S., Synthesis and Characterization of Thermosensitive Gelatin Hydrogel Microspheres in a Microfluidic System. *Macromol. Res.* **2016,** *24* (6), 529-536.

5. Allazetta, S.; Cosson, S.; Lutolf, M. P., Programmable Microfluidic Patterning of Protein Gradients on Hydrogels. *Chem. Commun. (Camb)* **2011,** *47* (1), 191-193.

6. Akbari, S.; Pirbodaghi, T., A Droplet-based Heterogeneous Immunoassay for Screening Single Cells Secreting Antigen-Specific Antibodies. *Lab Chip* **2014,** *14* (17), 3275-3280.

7. Velasco, D.; Tumarkin, E.; Kumacheva, E., Microfluidic Encapsulation of Cells in Polymer Microgels. *Small* **2012,** *8* (11), 1633-1642.

8. Chung, B. G.; Lee, K. H.; Khademhosseini, A.; Lee, S. H., Microfluidic Fabrication of Microengineered Hydrogels and their Application in Tissue Engineering. *Lab Chip* **2012,** *12* (1), 45-59.

9. Baker, S. N.; Baker, G. A., Luminescent Carbon Nanodots: Emergent Nanolights. *Angew. Chem., Int. Ed. Engl.* **2010,** *49* (38), 6726-6744.

10. Lee, C.; Pant, B.; Alam, A. M.; An, T.; Chung, H. J.; Hong, S. T.; Park, S. J.; Park, M.; Kim, H. Y., Biocompatible and Photoluminescent Keratin/Poly(vinyl alcohol)/Carbon Quantum Dot Nanofiber: A Novel Multipurpose Electrospun Mat. *Macromol. Res.* **2016,** *24* (10), 924-930.

11. Jun Zhang, C. L., Wenzhi Zhao, Baocang Liu, Yunxia Liu and Gaole Aletan, Biosensing Based on Luminescent Semiconductor Quantum Dots and Rare Earth Up-conversion Nanoparticles. **2011**.

12. Goncalves, H. M.; Duarte, A. J.; Esteves da Silva, J. C., Optical Fiber Sensor for Hg(II) Based on Carbon Dots. *Biosens. Bioelectron.* **2010,** *26* (4), 1302-1306.

13. Chen, Y. J.; Yang, Q.; Xu, P. P.; Sun, L.; Sun, D.; Zhuo, K. L., One-Step Synthesis of Acidophilic Highly-Photoluminescent Carbon Dots Modified by Ionic Liquid from Polyethylene Glycol. *Acs Omega* **2017,** *2* (8), 5251-5259.

14. Xu, X.; Ray, R.; Gu, Y.; Ploehn, H. J.; Gearheart, L.; Raker, K.; Scrivens, W. A., Electrophoretic Analysis and Purification of Fluorescent Single-Walled Carbon Nanotube Fragments. *J. Am. Chem. Soc.* **2004,** *126* (40), 12736-12737.

15. Hu, S. L.; Liu, J.; Yang, J. L.; Wang, Y. Z.; Cao, S. R., Laser Synthesis and Size Tailor of Carbon Quantum Dots. *J. Nanopart. Res.* **2011,** *13* (12), 7247-7252.

16. Ray, S. C.; Saha, A.; Jana, N. R.; Sarkar, R., Fluorescent Carbon Nanoparticles: Synthesis, Characterization, and Bioimaging Application. *J. Phys. Chem. C* **2009,** *113* (43), 18546-18551.

17. Tian, L.; Ghosh, D.; Chen, W.; Pradhan, S.; Chang, X. J.; Chen, S. W., Nanosized Carbon Particles From Natural Gas Soot. *Chem. Mater.* **2009,** *21* (13), 2803-2809.

18. Roy, P.; Chen, P. C.; Periasamy, A. P.; Chen, Y. N.; Chang, H. T., Photoluminescent Carbon Nanodots: Synthesis, Physicochemical Properties and Analytical Applications. *Mater. Today* **2015,** *18* (8), 447-458.

19. Bao, L.; Zhang, Z. L.; Tian, Z. Q.; Zhang, L.; Liu, C.; Lin, Y.; Qi, B.; Pang, D. W., Electrochemical Tuning of Luminescent Carbon Nanodots: From Preparation to Luminescence Mechanism. *Adv. Mater.* **2011,** *23* (48), 5801-5806.

20. Strauss, V.; Margraf, J. T.; Dolle, C.; Butz, B.; Nacken, T. J.; Walter, J.; Bauer, W.; Peukert, W.; Spiecker, E.; Clark, T.; Guldi, D. M., Carbon Nanodots: Toward a Comprehensive Understanding of Their Photoluminescence. *J. Am. Chem. Soc.* **2014,** *136* (49), 17308-17316.

21. Zhu, H.; Wang, X.; Li, Y.; Wang, Z.; Yang, F.; Yang, X., Microwave Synthesis of Fluorescent Carbon Nanoparticles with Electrochemiluminescence Properties. *Chem. Commun. (Camb)* **2009,** (34), 5118-5120.

22. Zhu, S.; Meng, Q.; Wang, L.; Zhang, J.; Song, Y.; Jin, H.; Zhang, K.; Sun, H.; Wang, H.; Yang, B., Highly Photoluminescent Carbon Dots for Multicolor Patterning, Sensors, and Bioimaging. *Angew. Chem., Int. Ed. Engl.* **2013,** *52* (14), 3953-3957.

23. Zhang, W. X.; Dai, D. J.; Chen, X. F.; Guo, X. X.; Fan, J. Y., Red Shift in the Photoluminescence of Colloidal Carbon Quantum Dots induced by Photon Reabsorption. *Appl. Phys. Lett.* **2014,** *104* (9), 091902.

24. Krysmann, M. J.; Kelarakis, A.; Dallas, P.; Giannelis, E. P., Formation Mechanism of Carbogenic Nanoparticles with Dual Photoluminescence Emission. *J. Am. Chem. Soc.* **2012,** *134* (2), 747-750.

25. Baptista, F. R.; Belhout, S. A.; Giordani, S.; Quinn, S. J., Recent Developments in Carbon Nanomaterial Sensors. *Chem. Soc. Rev.* **2015,** *44* (13), 4433-4453.

26. Chen, L.; Hwang, E.; Zhang, J., Fluorescent Nanobiosensors for Sensing Glucose. *Sensors (Basel)* **2018,** *18* (5), 1440.

27. López, C.; Cavaco-Paulo, A., In-situ Enzymatic Generation of Hydrogen Peroxide for Bleaching Purposes. *Eng. Life Sci.* **2008,** *8* (3), 315-323.

28. Wang, J. M.; Li, Y.; Wang, X. Y.; Wang, J. C.; Tian, H. M.; Zhao, P.; Tian, Y.; Gu, Y. M.; Wang, L. Q.; Wang, C. Y., Droplet Microfluidics for the Production of Microparticles and Nanoparticles. *Micromachines* **2017,** *8* (1), 22.

29. Teh, S. Y.; Lin, R.; Hung, L. H.; Lee, A. P., Droplet Microfluidics. *Lab Chip* **2008,** *8* (2), 198-220.

30. Joensson, H. N.; Andersson Svahn, H., Droplet Microfluidics—A Tool for Single-Cell Analysis. *Angew. Chem., Int. Ed.* **2012,** *51* (49), 12176-12192.

31. Hu, H. R.; Wang, H. T.; Du, Q. G., Preparation of pH-Sensitive Polyacrylic Acid Hollow Microspheres and their Release Properties. *Soft Matter* **2012,** *8* (25), 6816-6822.

32. Qu, D.; Zheng, M.; Zhang, L.; Zhao, H.; Xie, Z.; Jing, X.; Haddad, R. E.; Fan, H.; Sun, Z., Formation Mechanism and Optimization of Highly Luminescent N-doped Graphene Quantum Dots. *Sci. Rep.* **2014,** *4*, 5294.

33. Bui, T. T.; Park, S.-Y., A Carbon Dot–Hemoglobin Complex-Based Biosensor for Cholesterol Detection. *Green Chem.* **2016,** *18* (15), 4245-4253.

34. Cho, M. J.; Park, S. Y., Preparation of Poly(styrene)-b-poly(acrylic acid)-Coupled Carbon Dots and Their Applications. *ACS Appl. Mater. Interfaces* **2017,** *9* (28), 24169-24178.

35. Sharma, A. C.; Jana, T.; Kesavamoorthy, R.; Shi, L.; Virji, M. A.; Finegold, D. N.; Asher, S. A., A general Photonic Crystal Sensing Motif: Creatinine in Bodily Fluids. *J. Am. Chem. Soc.* **2004,** *126* (9), 2971-2977.

36. Magalhaes, A. S. G.; Neto, M. P. A.; Bezerra, M. N.; Ricardo, N. M. P. S.; Feitosa, J. P. A., Application of Ftir in the Determination of Acrylate Content in Poly(Sodium Acrylate-Co-Acrylamide) Superabsorbent Hydrogels. *Quim. Nova* **2012,** *35* (7), 1464-1467.

37. Kirwan, L. J.; Fawell, P. D.; van Bronswijk, W., In situ FTIR-ATR Examination of Poly(acrylic acid) Adsorbed onto Hematite at Low pH. *Langmuir* **2003,** *19* (14), 5802-5807.

38. Kalaivani, D.; Arthi, D.; Mukunthan, A.; Jayaraman, D.; Joseph, V., Growth and Characterization of L-Lysinium Succinate Single Crystal. *J. Cryst. Growth* **2015,** *426*, 135-140.

39. Moreno-Couranjou, M.; Mauchauffe, R.; Bonot, S.; Detrembleur, C.; Choquet, P., Anti-Biofouling and Antibacterial Surfaces via a Multicomponent Coating Deposited from an Up-Scalable Atmospheric-Pressure Plasma-Assisted CVD Process. *J. Mater. Chem. B* **2018,** *6* (4), 614-623.

40. Shrivastava, A.; Gupta V. B., Methods for the Determination of Limit of Detection and Limit of Quantitation of the Analytical Methods. *Chron. Young Sci.* **2011**, 2, 21-25.

41. Khan, M.; Park, S. Y., Liquid Crystal-Based Biosensor with Backscattering interferometry: A Quantitative Approach. *Biosens. Bioelectron.* **2017,** *87*, 976-983.

TOC

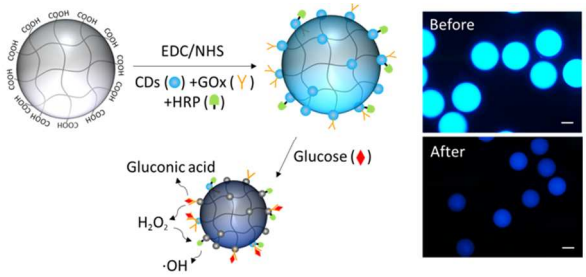
EDC/NHS
CDs ( ) +GOx ( )
+HRP ( )
Gluconic acid
Glucose ( )
H_2O_2
·OH
Before
After